JOC Article

Comparative Study of the Photochemistry of the Azidopyridine 1-Oxides

Kyle N. Crabtree,[†] Katherine J. Hostetler,[†] Tamara E. Munsch,[‡] Patrik Neuhaus,[‡] Paul M. Lahti,[§] Wolfram Sander,[‡] and James S. Poole*,[†]

Department of Chemistry, Ball State University, Muncie, Indiana 47306, Lehrstuhl für Organische Chemie II, Ruhr-Universität Bochum, D-44780 Germany, and Department of Chemistry, University of Massachusetts, Amherst, Massacusetts 01003

jspoole@bsu.edu

Received January 31, 2008

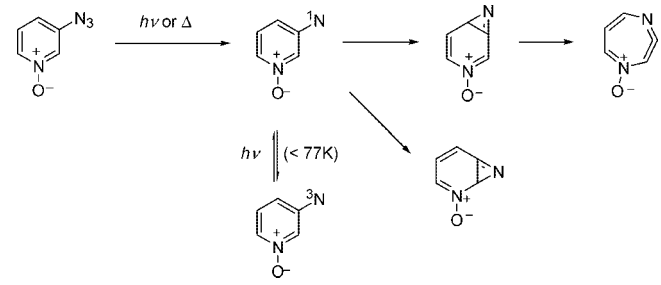

The photochemistry of azidopyridine 1-oxides was studied using an array of glass and matrix isolation techniques. As with room temperature, the photochemistry of 4-azidopyridine 1-oxide is dominated by triplet nitrene chemistry. However, in the case of the 3-azide, matrix photolysis indicates the formation of diazabicyclo[4.1.0]hepta-2,4,6-triene *N*-oxide and diazacycloheptatetraene *N*-oxide intermediates as well as triplet nitrene.

Introduction

The chemistry of aryl azides has received a great deal of attention due to their ability to undergo 1,3-dipolar cycloaddition reactions and their ability to act as thermo- and photochemical precursors of aryl nitrene species. Much of aryl nitrene chemistry has been concerned with the utilization of such species as bioaffinity labels[1] or as potential conductor materials,[2] although these nitrenes may also be synthetically useful in the formation of azepine[3] and carbazole[4] systems. The photochemistry of simple aryl azides is now well-established and has been the subject of recent reviews by Platz et al.[5,6] Using phenyl azide as an exemplar, the salient features of aryl nitrene photochemistry are shown in Scheme 1.

SCHEME 1. Photochemistry of Phenyl Azide

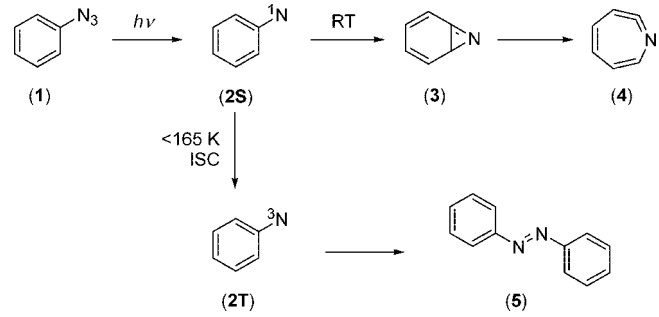

Photodecomposition of the aryl azide yields a singlet nitrene species **2S**, which at room temperature undergoes a ring-closure/ring-expansion sequence to yield the didehydroazepine **4**, for which a significant body of experimental evidence exists. The

[†] Ball State University.
[‡] Ruhr Universität Bochum.
[§] University of Massachusetts.

(1) (a) Meisenheimer, K. M.; Koch, T. H. *Crit. Rev. Biochem. Mol. Biol.* **1997**, *32*, 101. (b) Schnapp, K. A.; Platz, M. S. *Bioconjugate Chem.* **1993**, *4*, 178. (c) Schnapp, K. A.; Poe, R.; Leyva, E.; Soundararajan, N.; Platz, M. S. *Bioconjugate Chem.* **1993**, *4*, 172.

(2) Meijer, E. W.; Nijhuis, S.; van Vroonhoven, F.C.B.M. *J. Am. Chem. Soc.* **1998**, *110*, 7209.

(3) Doering, W.; Odum, R. A. *Tetrahedron* **1966**, *22*, 81.

(4) (a) For example, see: Swenton, J.; Ikeler, T.; Williams, B. *J. Am. Chem. Soc.* **1970**, *92*, 3103. (b) Tsao, M-L.; Gritsan, N. P.; James, T. R.; Platz, M. S.; Hrovat, D. A.; Borden, W. T. *J. Am. Chem. Soc.* **2003**, *125*, 9343.

(5) PlatzM.J. In*Reactive Intermediate Chemistry*;Moss,R.A.,Platz,M.S.,Jones,M., Jr., Eds.; John Wiley & Sons:Hoboken, NJ,2004; pp 522–546..

(6) Gritsan, N. P.; Platz, M. S. *Chem. Rev.* **2006**, *106*, 3844.

10.1021/jo8001936 CCC: $40.75 © 2008 American Chemical Society
Published on Web 04/10/2008

TABLE 1. Summary of Calculated Data for 4-Nitrenopyridine 1-Oxide and Photoproducts

method	B3LYP/6-31G*			CASSCF(8,8)/6-31G*			CASSCF(10,9)/6-31G*		CASSCF(8,8) MP2/6-31G*	
geometry	B3LYP/6-31G*			CASSCF(8,8)/6-31G*			CASSCF(8,8)/6-31G*		CASSCF(8,8)/6-31G*	
species	energy (hartree)	ZPE[a] (hartree)	$E_{rel,0K}$[b] (kcal/mol)	energy (hartree)	ZPE[c](hartree)	$E_{rel,0K}$[d] (kcal/mol)	energy (hartree)	$E_{rel,0K}$[d] (kcal/mol)	energy (hartree)	$E_{rel,0K}$[d] (kcal/mol)
7T	−377.5166	0.08422	−9.8	−375.3795	0.08874	−5.4	−375.3849	−6.5	−376.3426	−8.2
7S	−377.5010[f]	0.08429[f]	0.0[e,f]	−375.3706	0.08852	0.0[e]	−375.3744	0.0[e]	−376.3294	0.0[e]
TS (**7S**−**8**)	−377.4614	0.08328	24.2	−375.3314	0.08751	24.0	−375.3371	22.7	−376.3031	15.9
8	−377.4691	0.08419	19.9	−375.3344	0.08870	22.9	−375.3393	22.1	−376.3065	14.5
TS (**8**−**9**)	−377.4564	0.08251	26.9	−375.2945	0.08696	46.8	−375.3015[g]	44.7[g]	−376.2689	37.0
9	−377.4780	0.08432	14.4	−375.3338	0.088587	23.2	−375.3388	22.4	−376.3096	12.5

[a] Unscaled ZPE energies, [b] Determined using ZPE scaled by the factor recommended by Scott and Radom, ref 23. [c] Unscaled ZPE energies calculated at CAS(8,8)/6-31G*level of theory. [d] Determined using unscaled ZPE corrections calculated at CASSCF(8,8)/6-31G*level of theory. [e] Energies for each species are determined relative to the energy of the singlet nitrene **7S** (relative energy defined as 0). [f] Energies of singlet nitrenes are estimated from DFT calculations using the sum method described by Johnson et al., ref 16. [g] See the Supporting Information.

TABLE 2. Summary of Calculated Data for 3-Nitrenopyridine-1-Oxide and Photoproducts

method	B3LYP/6-31G*			CASSCF(8,8)/6-31G*			CASSCF(10,9)/6-31G*		CASSCF(8,8) MP2/6-31G*	
geometry	B3LYP/6-31G*			CASSCF(8,8)/6-31G*			CASSCF(8,8)/6-31G*		CASSCF(8,8)/6-31G*	
species	energy (hartree)	ZPE[a] (hartree)	$E_{rel,0K}$[b] (kcal/mol)	energy (hartree)	ZPE[c] (hartree)	$E_{rel,0K}$[d] (kcal/mol)	energy (hartree)	$E_{rel,0K}$[d] (kcal/mol)	energy (hartree)	$E_{rel,0K}$[d] (kcal/mol)
12T	−377.5004	0.08359	−16.4	−375.3659	0.08754	−17.2	−375.3706	−16.8	−376.3274	−15.4
12S	−377.4741[e,f]	0.08330[e,f]	0.0[e,f]	−375.3375	0.08660	0.0[e]	−375.3429	0.0[e]	−376.3019	0.0[e]
TS (**12S**−**13a**)	−377.4483[g]	0.08325[g]	16.1[g]	−375.3257	0.08683	7.5	−375.3314	7.4	−376.2949	4.6
TS (**12S**−**13b**)				−375.3266	0.08672	7.0	−375.3320	6.9	−376.2932	5.5
13a	−377.4713	0.08441	2.4	−375.3339	0.08898	3.7	−375.3394	3.7	−376.3077	−2.1
13b	−377.4840	0.08491	−5.3	−375.3426	0.08976	−1.2	−375.3484	−1.5	−376.3146	−6.0
TS (**13a**−**14a**)	−377.4627	0.08283	6.8	−375.2965	0.08708	26.0	−375.3019	26.1	−376.2759	16.6
TS(**13b**−**14b**)	−377.4638	0.08277	6.1	−375.2994	0.08723	24.3	−375.3046	24.4	−376.2825	12.6
14a	−377.4853	0.08460	−6.3	−375.3368	0.08897	1.9	−375.3430	1.4	−376.3117	−4.7
14b	−377.4749	0.08403	−0.1	−375.3316	0.08824	4.7	−375.3354	5.7	−376.3033	0.1

[a] Unscaled ZPE energies, [b] Determined using ZPE scaled by the factor recommended by Scott and Radom, ref 23. [c] Unscaled ZPE energies calculated at CAS(8,8)/6–31G* level of theory, [d] Determined using unscaled ZPE corrections calculated at CASSCF(8,8)/6–31G* level of theory. [e] Energies for each species are determined relative to the energy of the singlet nitrene **12S** (Rel. energy defined as 0). [f] Energies of singlet nitrenes are estimated from DFT calculations using the sum method described by Johnson et al., ref 19. [g] The transition state found can serve both reaction paths as the imaginary frequency corresponds to an out-of-plane N vibration. However, given the nature of the computational method it cannot necessarily be described as a true bifurcation point, and the CASSCF calculations bear this out.

SCHEME 2. Potential Photoproducts of 4-Azidopyridine 1-Oxide (6)

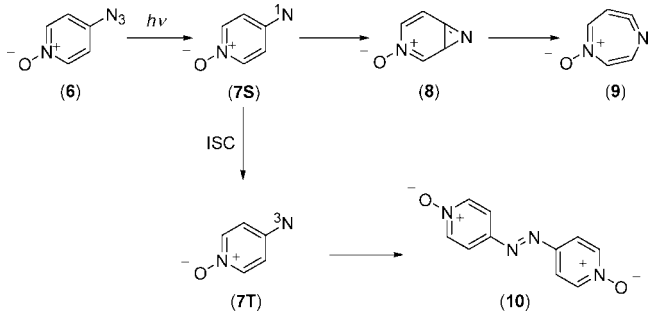

benzazirine **3** has not been observed for phenylnitrene[6] but has been observed in polycyclic arylnitrenes.[7] The ketenimine **4** is susceptible to nucleophilic attack, and this reaction may be used synthetically to yield amino- and alkylthioazepines.[3,8] At low temperatures (<165 K), intersystem crossing to the ground-state triplet is dominant,[9] and azobenzene (**5**) is observed as the dominant product.

A subclass of the aryl azides, the azidoheteroaryl *N*-oxides, has also received attention due to the potential of these compounds as antitumor agents.[10] In terms of the nitrene chemistry of such compounds, the presence of the *N*-oxide group would be expected to enhance the water solubility of these prospective bioaffinity agents, and provide opportunities for novel photochemistry from the *N*-oxide moiety, which is known to be photoreactive. Earlier product studies of the simplest of these compounds, the azidopyridine *N*-oxides, found that in the case of 2-azidopyridine 1-oxide, ring contraction to yield cyanopyrrole derivatives was particularly facile, and had demonstrable synthetic potential.[11] On the other hand, product studies following thermal and photochemical decomposition of 3- and 4-azidopyridine 1-oxide in organic solvents indicated that the products were predominantly polymeric and uncharacterizable in nature, and the majority of isolable and characterizable material could not be unambiguously identified as being derived from nitrene chemistry.[12]

In a recent paper, the photochemistry of 4-azidopyridine 1-oxide (**6**) was studied using transient spectroscopic techniques

(7) (a) Tsao, M.-L.; Platz, M. S. *J. Phys. Chem. A* **2004**, *108*, 1169. (b) Dunkin, I. R.; Thomson, P. C. *J. Chem. Soc., Chem. Commun.* **1980**, *499*. (c) Schrock, A. K.; Schuster, G. B. *J. Am. Chem. Soc.* **1984**, *106*, 5234. (d) Motawietz, J.; Sander, W. *J. Org. Chem.* **1996**, *61*, 4351.

(8) (a) DeGraff, B. A.; Gillespie, D. W.; Sundberg, *J. Am. Chem. Soc.* **1974**, *96*, 7491. (b) Carroll, S. E.; Nay, B.; Scriven, E. F. V.; Suschitzky, H.; Thomas, D. R. *Tetrahedron Lett.* **1977**, 3175.

(9) (a) For examples, see: Gritsan, N. P.; Godmundsdottir, A. D.; Tigelaar, D.; Platz, M. S. *J. Phys. Chem. A* **1999**, *103*, 3458. (b) Gritsan, N. P.; Tigelaar, D.; Platz, M. S. *J. Phys. Chem. A* **1999**, *103*, 4465.

(10) (a) Itai, T.; Kamiya, S. *Chem. Pharm. Bull.* **1961**, *9*, 87. (b) Itai, T.; Kamiya, S. *Chem. Pharm. Bull.* **1963**, *11*, 348. (c) Itai, T.; Kamiya, S. *Chem. Pharm. Bull.* **1963**, *11*, 1059.

(11) (a) Abramovitch, R. A., Jr *J. Org. Chem.* **1973**, *38*, 173. (b) Abramovitch, R. A., Jr *J. Am. Chem. Soc.* **1976**, *98*, 1478.

(12) Abramovitch, R. A.; Bachowska, B.; Tomasik, P. *Pol. J. Chem.* **1984**, *58*, 805.

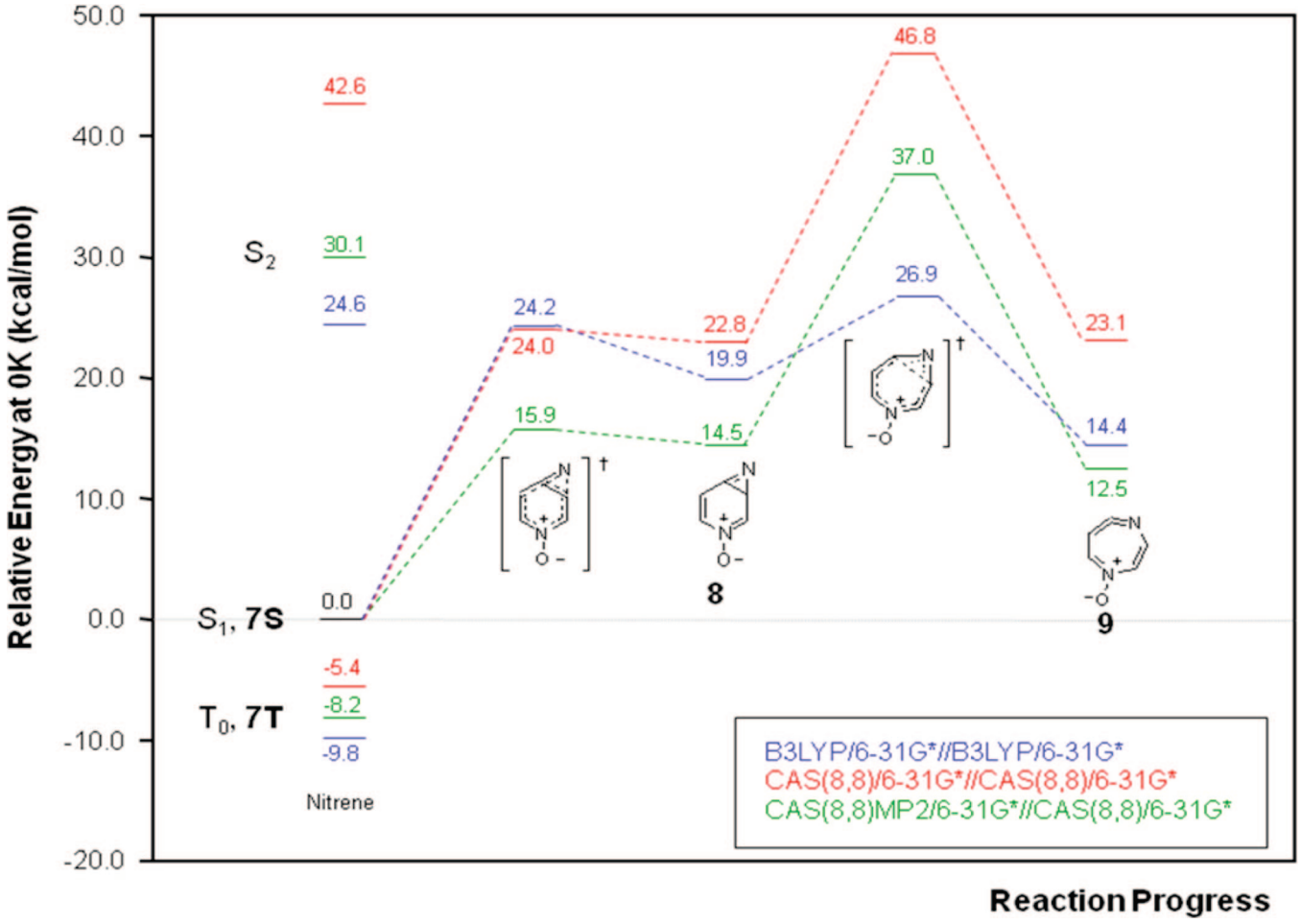

FIGURE 1. Reaction profile for 4-nitrenopyridine 1-oxide (**7**) calculated at various levels of theory. All energies are calculated at 0 K, relative to the energy of the nitrene S_1 state. ZPE corrections are employed.

(Scheme 2).[13] The authors reported that even at room temperature, the photochemistry of this compound was dominated by triplet nitrene chemistry—the only observed product was 4,4′-azobis(pyridine 1-oxide), **10**, and no evidence of products derived from **9** was found.

The explanation for this behavior was a selective stabilization of the S_1 state of the nitrene (**7S**), leading to enhanced rate of intersystem crossing to the triplet (**7T**) and a significant increase in the energetic barrier for cyclization to 3,7-diazabicyclo[4.1.0]hepta-2,4,6-triene 3-oxide, **8**. In the same way, it is sometimes convenient to consider **2S** as a biradical species, so it may also be useful to consider **7S** as an iminyl−aminoxyl biradical species. The aminoxyl character is a stabilizing influence: aminoxyls themselves have long been known to be stable (or persistent) free radicals,[14] and similar stabilizing effects may be used to explain the "super-stabilizing" effect the 4-(pyridine 1-oxide) group has on radical species, as demonstrated by Creary.[15]

In the case of 3-azidopyridine 1-oxide (**11**) and its resultant nitrenes (**12S/T**), the positioning of the two groups does not allow the "super-stabilizing" effect, and we might anticipate that these nitrenes would exhibit chemical behavior qualitatively similar to **2S/T**.

In this contribution, we report on a combined computational and low-temperature spectroscopic study of the photochemistry of **6** and **11**.

Results and Discussion

Theoretical Calculations. Summaries of calculated energies for critical points along the reaction paths of 4-nitrenopyridine 1-oxide (**7**) and 3-nitrenopyridine 1-oxide (**12**) are shown in Tables 1 and 2 respectively, and graphical representations of the various reaction paths are shown in Figures 1 and 2.

Each of the methods used in this study have their strengths and weaknesses, which have been alluded to in previous studies.[16,17] The DFT methodology, as utilized in GAUSSIAN, cannot readily calculate the properties of open shell singlet states—it is necessary to use approximate sum methods to predict the energy of aryl nitrene S_1 states because of this fact. In addition, the transition states for cyclization to the benzazirine analogues are likely to retain a significant amount of open-shell character, so we cannot expect DFT methods to perform well

(13) Hostetler, K. J.; Crabtree, K. N.; Poole, J. S. *J. Org. Chem.* **2006**, *71*, 9023.

(14) (a) Mahoney, L. R.; Mendenhall, G. D.; Ingold, K. U. *J. Am. Chem. Soc.* **1973**, *95*, 8610. (b) Lebedev, Y. A.; Rozantsev, E. G.; Kalashnikova, L. A.; Lebedev, V. P.; Neiman, M. B.; Apin, A. Y. *Dokl. Akad. Nauk SSSR (Engl.)* **1966**, *40*, 460.

(15) Creary, X. *Acc. Chem. Res.* **2006**, *39*, 761.

(16) Johnson, W. T. G.; Sullivan, M. B.; Cramer, C. J. *Int. J. Quantum Chem.* **2001**, *85*, 492.

(17) Karney, W. L.; Borden, W. T. *J. Am. Chem. Soc.* **1997**, *119*, 1378.

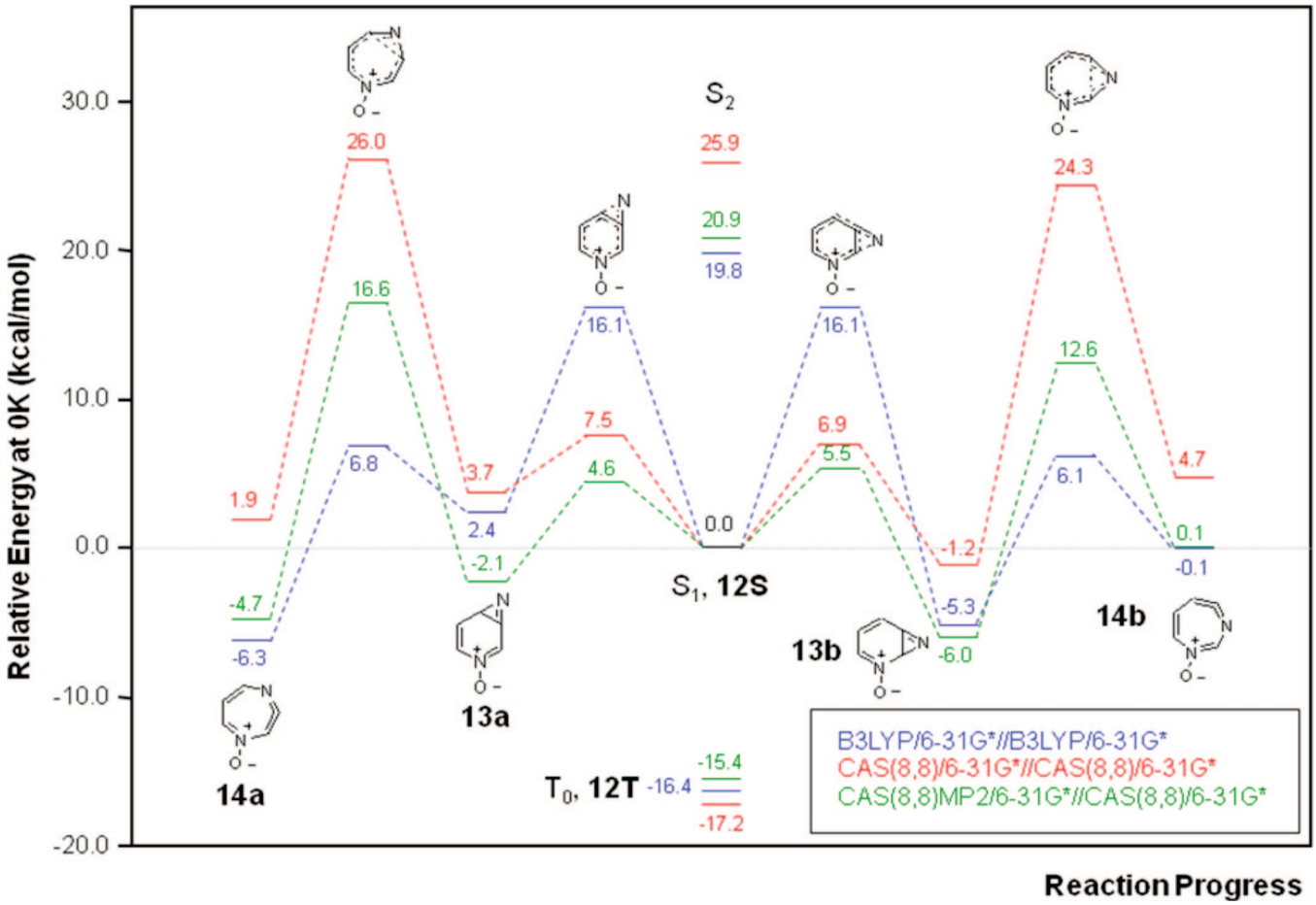

FIGURE 2. Reaction profile for 3-nitrenopyridine 1-oxide (**12**) calculated at various levels of theory. All energies are calculated at 0 K, relative to the energy of the nitrene S_1 state. ZPE corrections are employed.

for these transition states, and the CI approach of CASSCF calculations might be expected to be superior.

On the other hand, Karney and Borden[17] have demonstrated that the CASSCF approach tends to overestimate the energy of the transition state for ring opening from benzazirine to ketenimine for aryl nitrenes. The authors noted in their original study that dynamic electron correlation plays an important role in the transition states of pericyclic reactions such as these and employed Møller–Plesset perturbation corrections to account for this effect in the form of CASPT2 energies. In this study, we have utilized the CASSCF MP2 methodology included in the GAUSSIAN suite to achieve these ends. We would expect this type of calculation and DFT (which includes dynamic correlation in the formulation of its functionals) to provide more insight regarding the ring expansion step than CASSCF calculations alone. We have found with phenylnitrene (see the Supporting Information) that MP2 corrections to CASSCF wave functions provide a partial treatment of dynamic correlation, but not to the extent of CASPT2 models, and certainly not to the extent of DFT models such as B3LYP. Thus, it can be argued that B3LYP/6-31G* calculations provide a superior description of this part of the reaction profile diagram, and these calculations are therefore included.

With the above provisos in mind, we may consider the reaction pathways in Figures 1 and 2. Figure 1, which includes previously published DFT data, shows a number of consistencies for all data sets. The first is that E_{ST} for nitrene **7** is small (5–10 kcal/mol depending on method used) relative to the analogous value for phenylnitrene (19.1 kcal/mol, calculated at CASPT2/6-31G*),[17] both favoring the triplet. This will lead to the enhanced rate of ISC observed experimentally.[13] In addition, the cyclization reaction to **8** is energetically unfavorable; it has a large barrier to cyclization and a very small barrier to ring opening. While cyclization of aryl nitrenes to benzazirines is generally endoergic, what is interesting about this system is that 1,4-diazacyclohepta-2,4,5,7-tetraene 1-oxide (**9**), formed by ring expansion, is also an energetically unfavorable product. It is also noteworthy that for all of the methodologies utilized, the barrier to expansion from **8** to **9** exceeds the S_1-S_2 energy gap for **7**. The computed energies are consistent with experimental observations even at room temperature—the chemistry of **7** is triplet dominated, with no evidence of ring-expansion products. In a matrix, we would anticipate that the triplet nitrene **7T** would be the primary photoproduct and that not even sustained photolysis of **7T** would yield **9** (cf. phenylnitrene). Secondary photoproducts would either arise from triplet chemistry (e.g., hydrogen atom abstraction) or *N*-oxide photochemistry.[18]

When considering the possible fate of 3-nitrenopyridine 1-oxide (**12**), it is necessary to consider two possible cyclization/ring expansion pathways; one beginning with *N*-cyclization

(18) (a) Spence, G. G.; Taylor, E. C.; Buchardt, O. *Chem. Rev.* **1969**, *69*, 231. (b) Albini, A.; Alpegiani, M. *Chem. Rev.* **1984**, *84*, 43. (c) Shi, X.; Poole, J. S.; Emenike, I.; Burdzinski, G.; Platz, M. S. *J. Phys. Chem. A* **2005**, *109*, 1491.

SCHEME 3. Potential Photoproducts of 3-Azidopyridine 1-Oxide (11)

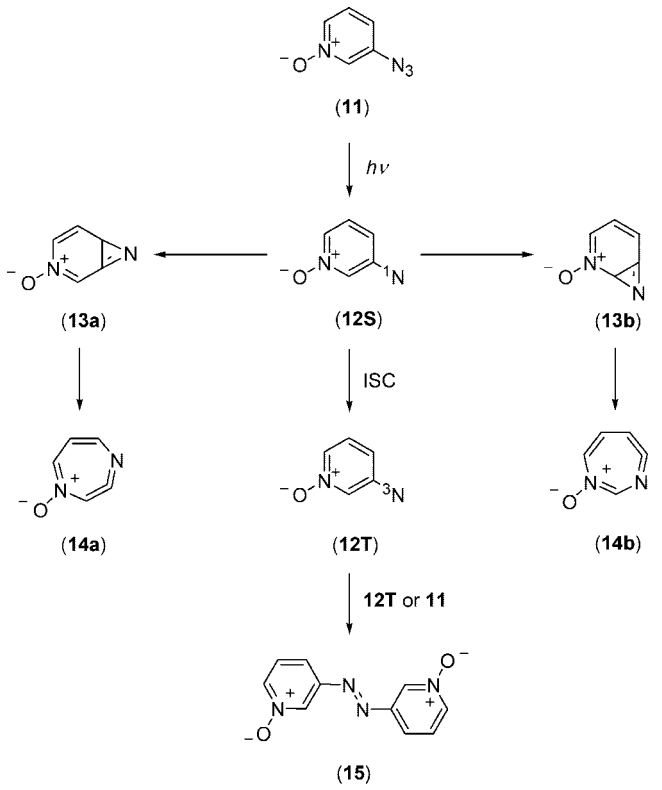

toward the *N*-oxide moiety (**12S** → **13b** → **14b**) and the other involving cyclization away from *N*-oxide (**12S** → **13a** → **14a**, see Scheme 3). The computational results are shown in Figure 2 and present some intriguing possibilities.

The first notable feature of this system is that the E_{ST} for **12** is estimated between 15 and 17 kcal/mol, favoring **12T**, a value quite similar to that of phenylnitrene. It is also worth noting that the calculations also indicate that the ability to delocalize spin density is a stabilizing effect: At the CASSCF (8,8) MP2/6-31G* level of theory, triplet 4-nitrenopyridine-1-oxide is some 9.5 kcal/mol more stable than the 3-nitreno isomer. The effect is even more pronounced in the open shell singlet state: the 4-nitrene is some 17 kcal/mol more stable than the 3-nitrene.

Based on the E_{ST} for **12**, we anticipate that at room temperature singlet nitrene chemistry will dominate, and we will only observe **15** at low temperatures, if at all. An interesting question regards what form the singlet nitrene chemistry will take. If we consider the pathway leading to **14a**, we see that it is similar to most reaction pathways of this type for simple aryl nitrenes: the nitrene **12S** overcomes a small barrier to generate 4,7-diazabicyclo[4.1.0]hepta-2,4,6-triene 4-oxide, **13a**, which is approximately isoenergetic (in aryl nitrene systems, the benzazirine intermediate is usually energetically less stable than the nitrene), and undergoes a rapid reaction to yield the energetically stable 1,4-diazacyclohepta-2,3,5,7-tetraene 1-oxide (**14a**).

However, if we consider the alternative pathway, we find that 1,3-diazacyclohepta-1,3,4,6-tetraene 1-oxide (**14b**) is approximately isoenergetic with **12S** and that the minimum energy structure for this reaction pathway is actually *2,7-diazabicyclo[4.1.0]hepta-2,4,6-triene 4-oxide* (**13b**). This finding represents an unusual case for simple aryl nitrenes and implies that in a low temperature matrix, photolysis of **11** will yield **12S**, which may undergo ISC to yield **12T**, or potentially generate **14a** and/or **13b** as secondary photoproducts. As with other aryl nitrenes, photolysis of **12T** will allow reaccess to the singlet surface via **12S** and may also result in the formation of **14a** and/or **13b**.

The thermochemical preference for **14a** and **13b** over their respective isomeric forms is worthy of comment, particularly with respect to the diazacycloheptatetraene *N*-oxides **14a** and **14b**. Some insight may be offered by considering the structures of the isomers, and their potential for conjugative interactions (Figure 3). All of the species shown in Figure 3 contain potentially conjugated π-systems as substructures, each constrained in terms of bond lengths by the fact that they reside within a six- or seven-membered ring. Two structural motifs are apparent: (i) an α,β-unsaturated imine substructure (C═C−C═N) observed in **13b** and **14a** and (ii)an *N*-vinylimine substructure (C═C−N═C) observed in **8**, **9**, **13a**, and **14b**.

In cases with the α,β-unsaturated imine substructure, the constraints of the ring geometry can also accommodate a significant degree of conjugation. The lengths for the C═C, C−C, and C═N bonds are 1.37, 1.43–1.44, and 1.35 Å, respectively, in **13b** and **14a**. Such bond lengths are consistent with the bond lengths observed in a conjugated diene such as 1,3-butadiene, allowing for the fact that C−N bond lengths are generally shorter than their C−C analogues.

On the other hand, species containing the *N*-vinylimine substructure have bond lengths that are not as accommodating toward conjugative overlap. In such species, the C−N bond lengths in these substructures vary between 1.44 and 1.45 Å. It is worth remembering that C−N bond lengths in simple alkylamines are of the order of 1.47 Å—it would therefore appear that the bond order for these C−N bonds is close to 1, and there is evidence of only a limited amount of the bond compression that one would associate with conjugation. Similarly, the bond lengths of the C═C and C═N fragments of the substructures are much closer to isolated double bond lengths than those found for **13b** and **14a**. The lower degree of conjugation in systems such as **13a** and **14b** is a significant contributor to the relative instabilities of these compounds relative to the conjugated isomeric forms **13b** and **14a**. The fact that neither **8** nor **9** apparently display significant conjugative stabilization, coupled with the high and selective stabilization (see above) of **7S**, indicates that ring expansion would not be favorable in the 4-nitreno system.

Electron Paramagnetic Resonance. EPR spectroscopy is the method where any "super-stabilizing" effect of the pyridine *N*-oxide moiety would manifest itself clearly in the zero field splittings (zfs) *D*/*hc* of **7T** and **12T**. A triplet nitrene with more delocalized π-spin density would have a smaller zfs interaction between its π-spin and localized σ-spin. Based on connectivity, a π-spin delocalized **7T** should have a smaller zfs interaction than **12T**, and the experimental data bear out this expectation (Table 3).[19]

The results of natural population analysis calculations for **7T** and **12T** at the B3LYP/6-31G* level of theory are shown in Figure 4. The results for **7T** indicate that there is a significant degree of spin density associated with the *N*-oxide moiety in this species (and hence delocalization of spin density for this species as a whole). This characteristic was not observed in **12T**, and these observations are consistent with our expectations for these species.

(19) For example, see: Dougherty, D. A. In *Kinetics and Spectroscopy of Carbenes and Biradicals* Platz, M. S., Eds.; Plenum Press: New York, 1990.

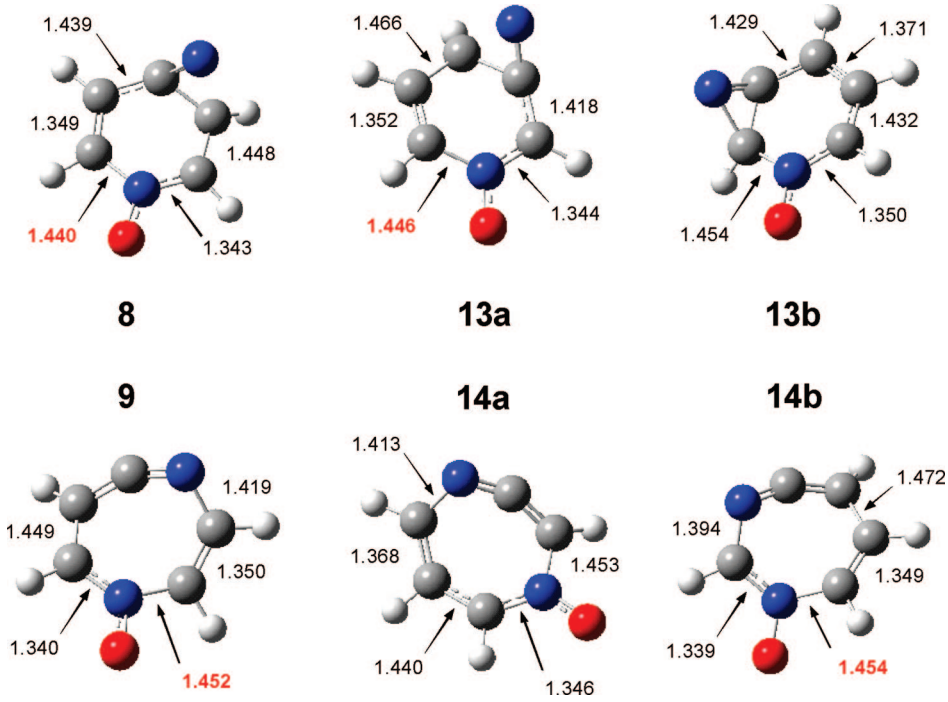

FIGURE 3. Optimized geometries for diazabicyclo[4.1.0]hepta-2,4,6-triene *N*-oxide and diazacycloheptatetraene *N*-oxide products of 3- and 4-nitrenopyridine 1-oxide, calculated at the B3LYP/6-31G* level of theory. All bond lengths in angstroms.

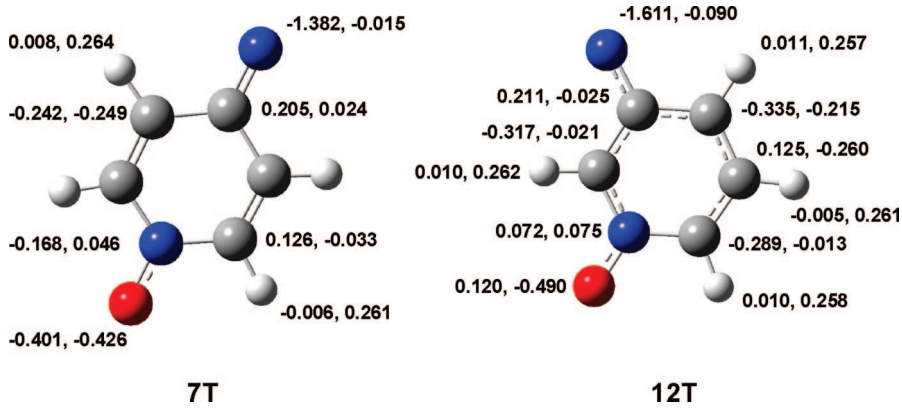

FIGURE 4. NPA spin and charge densities for **7T** and **12T**, calculated at the B3LYP/6-31G* level of theory. Spin densities are listed first, charge densities second.

TABLE 3. Summary of EPR Data for Triplet Nitrenes 7T and 12T

glass	4-nitrenopyridine 1-oxide (**7T**)		3-nitrenopyridine 1-oxide (**12T**)	
	D/*hc* (cm^{-1})	*E*/*hc* (cm^{-1})	*D*/*hc* (cm^{-1})	*E*/*hc* (cm^{-1})
95% ethanol	0.71 ±0.03[a]	<0.003	1.159	<0.004
2-methyltetrahydrofuran	0.746	<0.007	1.076	<0.003
toluene	0.700	0.006	1.060	0.003
Ar matrix	0.621[b,c]	0.003	1.054[c]	0.001

[a] The nitrene signal was distorted by overlap with a secondary signal of unknown origin. See the Supporting Information. [b] Broad band irradiation 295–320 nm. [c] Irradiation at 308 nm (Xe-Cl laser).

UV–vis Spectroscopy. The spectra obtained following photolysis of **6** and **11** in 3-methylpentane glasses are shown in Figure 5. The primary photoproduct observed on photolysis of **6** is the triplet nitrene **7T**, which exhibits a structured band at approximately 470–520 nm. A similar band has been observed at room temperature for this species in laser flash photolysis studies and is consistent with TD-DFT calculations, which predict a strongly absorbing band at 464 nm (in the gas phase).[13] Sustained photolysis of this species leads to a secondary photoproduct with a broad, unstructured band at approximately 340 nm. Minor shifts in the absorbance bands around 500 nm suggest that the secondary photoproduct may absorb in this region of the spectrum as well.

A scale-up experiment involving the photolysis of **6** in 200 mL of vitrified 3-methylpentane solution, followed by extraction with D_2O, gave a ^1H NMR spectrum consisting of three

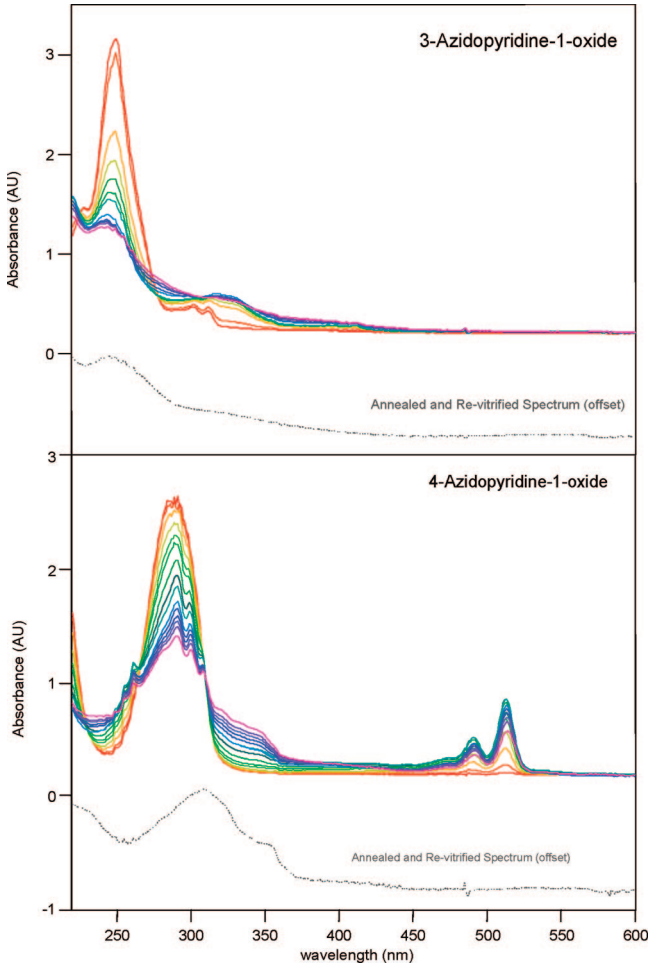

FIGURE 5. UV–vis spectra obtained during low temperature photolysis of **6** and **11** in 3-methylpentane at 77 K. Spectra were obtained at 30 s (red-light blue) and then 60 s (blue-violet) intervals for **6** and 15 s (red-light blue) and 60 s (blue-violet) intervals for **11**.

significant components: unreacted **6**, the azo-dimer **10**, and a third species which corresponded to 4-aminopyridine 1-oxide (**16**). The latter compound was isolated by preparative HPLC and characterized by ^{1}H and ^{13}C NMR: its structure was confirmed by comparison with an authentic sample.

The specific mechanism of formation of **16** is uncertain, but there are two plausible possibilities. The first involves the abstraction of hydrogen from solvent by the iminyl moiety, followed by disproportionation of the formed radical pair. A second possibility is similar but involves hydrogen abstraction from the aminoxyl moiety as an alternative step. Studies of persistent aminoxyl radicals[20] have found that the excited states of such species are highly adept at hydrogen abstraction, and so two separate hydrogen abstraction steps at the iminyl and aminoxyl sites of the triplet species, with rapid tautomerization once the glass melts (or during extraction into D_2O), is at least possible. Thus, in the absence of diazacycloheptatetraene *N*-oxide species (see below), the peaks observed at 340 and 500 nm in these glass experiments are due to a mixture of triplet nitrene and presumably a free radical intermediate formed as the result of hydrogen atom abstraction from the solvent by triplet nitrene.

(20) Bottle, S. E.; Chand, U.; Micallef, A. S. *Chem. Lett.* **1997**, 857.

Photolysis of argon matrix-isolated **6** at 450 nm yields qualitatively similar UV–vis spectra to the solution results, although the system of bands around 450–550 nm is somewhat more structured than those obtained in organic glasses (see the Supporting Information) and does not diminish over prolonged irradiation, presumably due to a lack of abstractable hydrogen in the argon matrix.

Photolysis of **11** in both organic glasses and argon matrix lead to broad, poorly structured spectra with peaks that are difficult to characterize and in all likelihood consist of spectra of more than one species (see discussion below). TD-DFT calculations for **12T** indicate that there is an allowed absorption at approximately 450–500 nm, but that this is significantly less intense than that of **7T** and is not observed experimentally. **12T** was calculated to be weakly absorbing, with maxima at approximately 300 and 260 nm. The broad unstructured bands observed at 340 and 380 nm are consistent with ketenimine species such as **14a** or **14b** (TD-DFT calculated absorbances around 280, 383 and 290, 335 nm, respectively). Species such as **13a** and **13b** were also calculated to have significant absorbances at 320 and 350 nm, respectively (see the Supporting Information. Matrix infrared experiments (see below) indicate the presence of a mixture of products following photolysis of **11**–**12T**, **13b**, and **14a**. The observed UV–vis spectra are consistent with such a mixture.

Matrix Infrared Spectroscopy. The difference spectrum obtained following photolysis of **6** in an argon matrix below 10 K is shown in Figure 6. A number of infrared absorbances of **6** exhibit multiple signals due to matrix site effects. Photolysis of the matrix at 308 nm generates a violet-colored species which may be identified as the triplet species **7T** by its observed color and by absorbances at 1583, 1395, 1150, 816, and 795 cm^{-1}, which are consistent with the calculated spectrum for this species (calculated at B3LYP/6-31G* level of theory, and scaled by a factor of 0.9614). Thus, the observation that **7T** is the dominant photoproduct in the matrix is consistent with observations in organic glasses (and for that matter, in solution at 298 K). There is no spectroscopic evidence to suggest the formation of either **8** or **9** in the matrix.

The matrix-isolated infrared spectra obtained after photolysis of **11** are a somewhat more complex matter, and prolonged irradiation or subsequent irradiation at alternate wavelengths is required to fully assign the spectral features of the photoproducts—in a number of cases, there is significant spectral overlap between species that can only be resolved by changes in photolysis conditions.

Initial photolysis of **11** in an argon matrix with 295–320 nm band radiation shows facile decomposition of the parent azide to yield a mixture of three products: **12T**, **14a**, and **13b**, indicated by characteristic absorbances at 1543, 1888, and 1713 cm^{-1}, respectively (see Figure 7). Further photolysis under these conditions leads to a decrease in **12T** and possibly in **14a**, with an increase in **13b**. On this basis, it is possible to partially assign bands in the infrared spectrum (see both Figure 7). However, there remain a number of bands that overlap, and so it is necessary to perform wavelength selective photolysis to assign the remaining bands.

Selective irradiation of the mixture of Figure 6 at 530–680 nm should lead to triplet photochemistry, since **12T** is the only species expected to absorb in this range (based on TD-DFT calculations). Indeed, photolysis in this wavelength range led to diminution of the bands assigned to triplet **12T**, with an

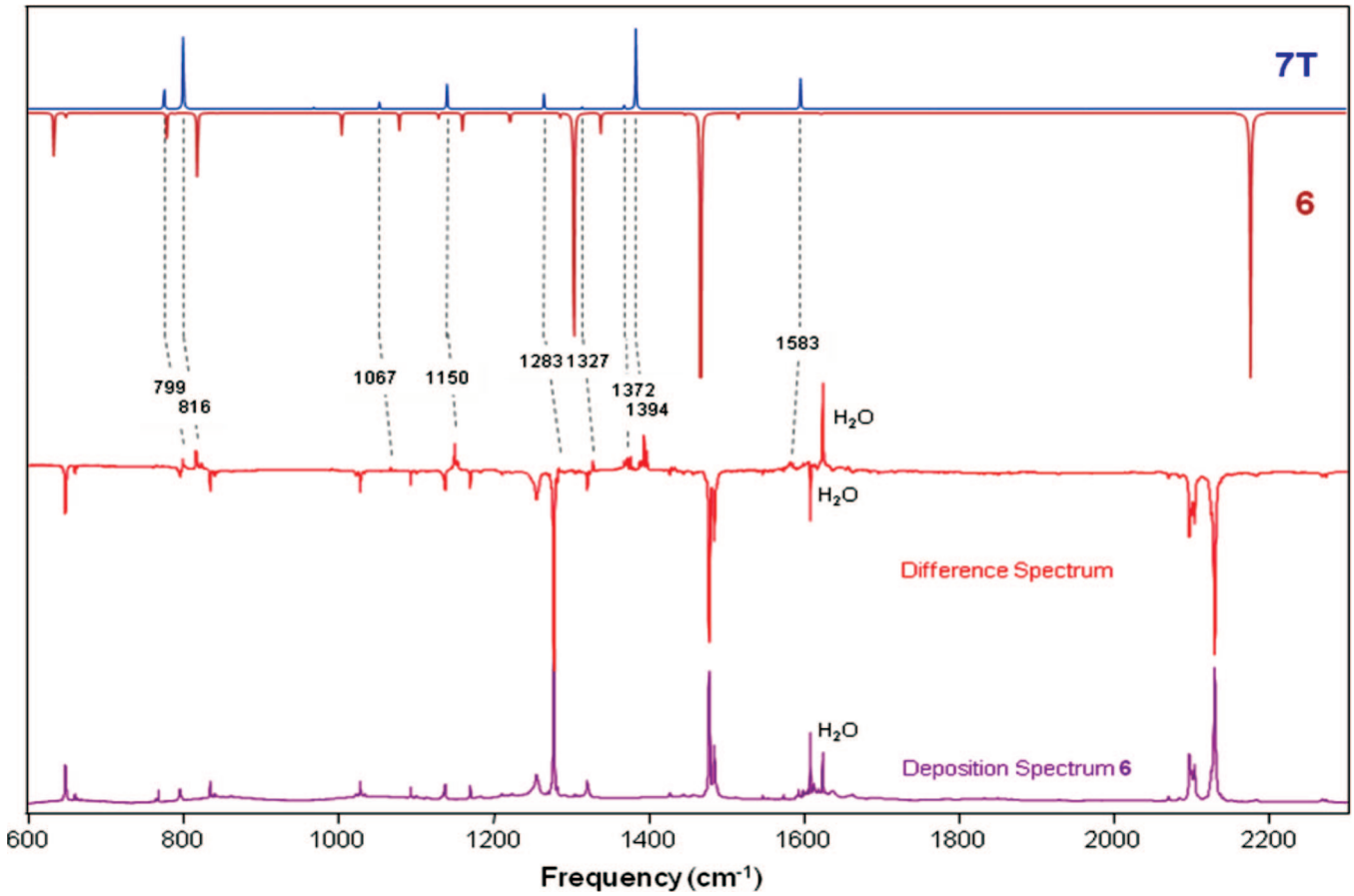

FIGURE 6. Differential IR spectrum following photolysis of **6** at 308 nm (red) in comparison with simulated spectra for **6** (brown) and **7T** (blue), calculated at the B3LYP/6-31G* level of theory. Peaks at 1608 and 1624 cm^{-1} correspond to matrix isolated H_2O codeposited with **6** (violet). Experimental vibrational frequencies for **7T** are shown.

increase those for **13b** and **14a**, thus allowing us to unambiguously assign the bands corresponding to **12T** (see Figure 8).

Further irradiation at 395–450 nm leads to a decrease in bands for **14a** and an increase in those for **12T** and possibly **13b** (based on a small increase in absorbance at 1715 cm^{-1}). Again, TD-DFT calculations indicate that **14a** will have appreciable absorbance in this wavelength range, but **12T** will absorb weakly in this range and **13b** will not absorb at all. These observations allow us to partially assign the remaining bands (Figures 7 and 8). The assignments for **12T** and **14a** are relatively unambiguous, but the assignment of the peaks for **13b** is less so, due to the high degree of spectral overlap.

The initial irradiation at 295–320 nm is nonselective: not only does the azide **11** absorb in this region of the spectrum, but so do the intermediates **12T**, **13b**, and **14a**. It appears from subsequent photolysis experiments that **12T** and **14a** may photochemically interconvert and that **14a** can be converted to **13b**. It has not been established whether **13b** will convert to **12T** or **14a**. It seems likely that the singlet nitrene **12S** represents a mechanistic branching point—it is difficult to visualize a simple mechanism for the conversion of **14a** to **13b** that does not proceed via a nitrene intermediate. In addition, it appears that **12T** acts as a photochemical "reservoir" for **12S** in these experiments.

The observed product distribution of **12T/13b/14a** in all likelihood arises out of a series of linked photostationary equilibria; and this tends to be confirmed by the fact that selective irradiation of certain isomers leads to a shift in the product distribution. However, where cyclization of **12S** occurs, the more stable isomers **13b** and **14a** are formed, but **14b** and **13a** are not. This suggests that **12S** is formed vibrationally "hot", and thermochemical equilibria of **13b/14b** and **13a/14a** may be established prior to relaxation/dissipation of vibrational energy into the matrix. Under such circumstances, we would observe the thermochemically stable species **13b** and **14a**.

Conclusions

It is clear that our previous description of 4-nitrenopyridine 1-oxide as an iminyl-aminoxyl biradical system is justified by the degree of spin delocalization deduced from the EPR spectrum of this species, relative to a "typical" aryl nitrene system. The chemistry of this species is dominated by triplet chemistry at low temperature and room temperature—we have been unable to observe any product that might arise from the singlet nitrene, and such behavior is borne out by calculations. The biradical nature of the intermediate makes photochemical hydrogen abstraction in organic glasses relatively facile.

In contrast, the radical "super-stabilizing" properties of the *N*-oxide group are not available to 3-nitrenopyridine 1-oxide, and so it behaves more like a typical aryl nitrene: the triplet state is obtained initially during low temperature photolysis, but the singlet state can be accessed upon prolonged photolysis, yielding products consistent with cyclization and ring expansion. This system is unusual, however, in that both of the two possible modes of cyclization are observed at low temperature; in one

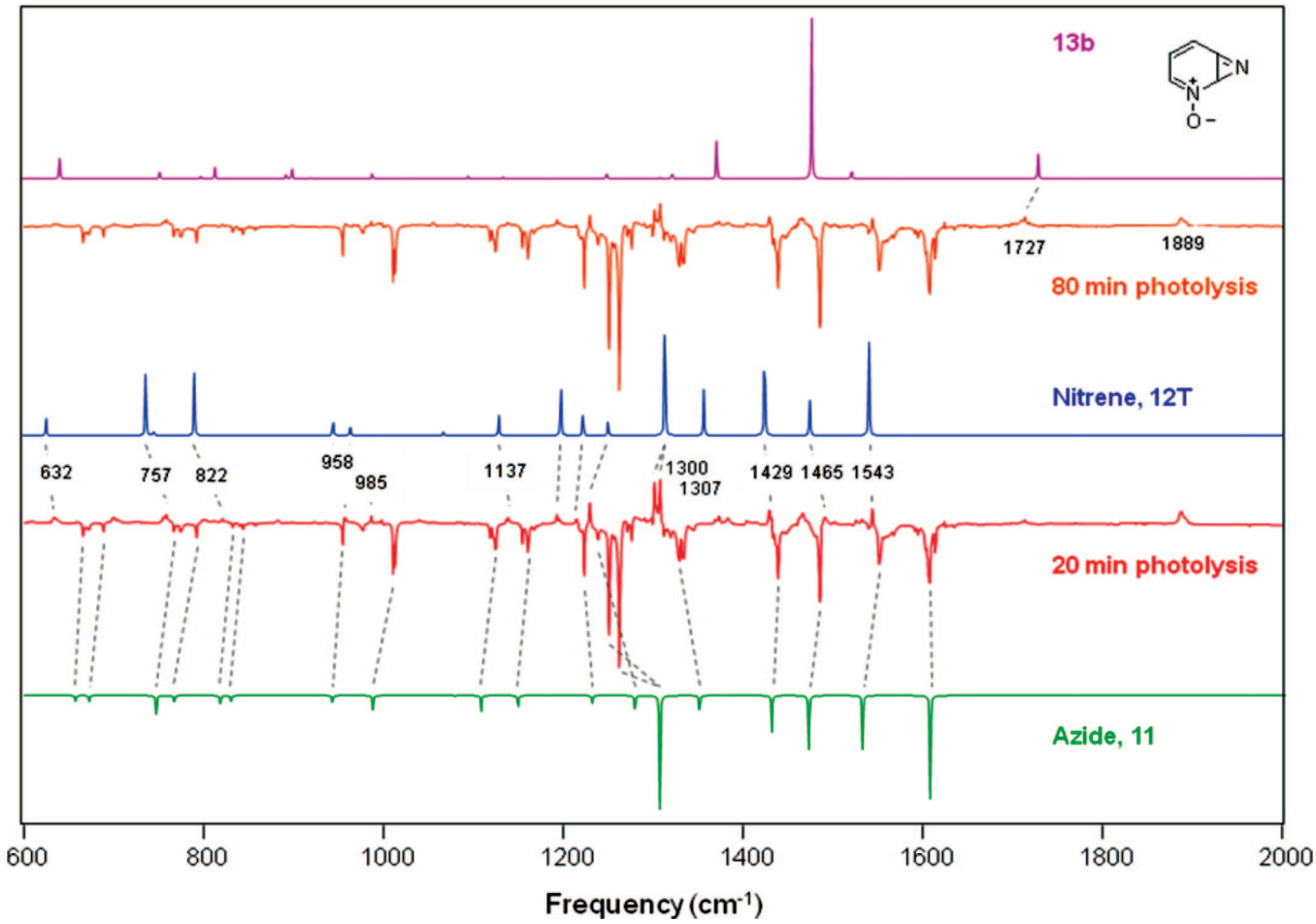

FIGURE 7. Differential IR spectra following Ar matrix photolysis of **11** at 295–320 nm (red and orange) in comparison with simulated spectra for **12T** (blue) **13b** (violet),and **11** (green), calculated at the B3LYP/6-31G* level of theory.

mode, the product is the expected diazacycloheptatetraene *N*-oxide; whereas in the other mode, the diazabicyclo[4.1.0]hepta-2,4,6-triene *N*-oxide intermediate is the favored species.

How do these studies relate to the solution studies performed by Abramowitz et al.,[12] who found no evidence of ring-expansion products when **11** was thermolyzed or photolyzed in the presence of nucleophiles? If we assume that the azide acts as a "normal" aryl azide, we would expect the formation of aminoazepine products in the presence of amines.[3] Our initial LFP experiments with **11** at room temperature indicate that photolysis of **11** in the absence of amine trap does yield polymeric material, and that the absorbance of the formed polymer can be quenched by the addition of diethylamine or dibutylamine as a trap. However, the trapped nitrene product (nominally the aminoazepine) itself is highly photolabile, and even exposure to moderate amounts of light leads to the formation of highly colored oligomeric materials. We note that previous workers did not obtain a great deal of characterizable material in their studies.[12] Further study is underway to further elucidate the room temperature chemistry of **11** with nucleophiles to determine the products generated and the photochemistry they undergo.

Computational Methodology

Density functional theory (DFT) calculations were performed using the GAUSSIAN 03 program suite.[21] Geometry optimizations and energies were performed at the B3LYP/6-31G* level of theory for all species,[22] and vibrational frequencies were calculated at the same level of theory, corrected by factors of 0.9614 (frequencies), 0.9806 (zero point energies), and 0.9989 (enthalpic corrections to 298 K) as recommended by Scott and Radom.[23] Transition states for nitrene and azide rearrangements were found to have a single imaginary frequency, corresponding to the appropriate reaction coordinate. The energetics of the open-shell singlet states of the nitrenes listed above were estimated according to the method of Johnson et al.,[16] whereby a UDFT optimization based on the RDFT nitrene wave function with promotion of a single electron into the

(21) Frisch, M. J.; Trucks, G. W.; Schlegel, H. B.; Scuseria, G. E.; Robb, M. A.; Cheeseman, J. R.; Montgomery, J. A., Jr.; Vreven, T.; Kudin, K. N.; Burant, J. C.; Millam, J. M.; Iyengar, S. S.; Tomasi, J.; Barone, V.; Mennucci, B.; Cossi, M.; Scalmani, G.; Rega, N.; Petersson, G. A.; Nakatsuji, H.; Hada, M.; Ehara, M.; Toyota, K.; Fukuda, R.; Hasegawa, J.; Ishida, M.; Nakajima, T.; Honda, Y.; Kitao, O.; Nakai, H.; Klene, M.; Li, X.; Knox, J. E.; Hratchian, H. P.; Cross, J. B.; Adamo, C.; Jaramillo, J.; Gomperts, R.; Stratmann, R. E.; Yazyev, O.; Austin, A. J.; Cammi, R.; Pomelli, C.; Ochterski, J. W.; Ayala, P. Y.; Morokuma, K.; Voth, G. A.; Salvador, P.; Dannenberg, J. J.; Zakrzewski, V. G.; Dapprich, S.; Daniels, A. D.; Strain, M. C.; Farkas, O.; Malick, D. K.; Rabuck, A. D.; Raghavachari, K.; Foresman, J. B.; Ortiz, J. V.; Cui,Q.; Baboul, A. G.; Clifford, S.; Cioslowski, J.; Stefanov, B. B.; Liu, G.; Liashenko, A.; Piskorz, P.; Komaromi,I.; Martin, R. L.; Fox, D. J.; Keith, T.; Al-Laham, M. A.; Peng, C. Y.; Nanayakkara, A.; Challacombe, M.; Gill, P. M. W.; Johnson, B.; Chen, W.; Wong, M. W.; Gonzalez, C.; Pople, J. A. *Gaussian 03, Revision C.02*,Gaussian, Inc.: Wallingford, CT, 2004.

(22) (a) Becke, A. D. *Phys. Rev. A* **1988**, *38*, 3098. (b) Becke, A. D. *J. Chem. Phys.* **1993**, *98*, 5648. (c) Lee, C.; Yang, W.; Parr, R. G. *Phys. Rev. B* **1988**, *37*, 785.

(23) Scott, A. P.; Radom, L. *J. Phys. Chem.* **1996**, *100*, 16502.

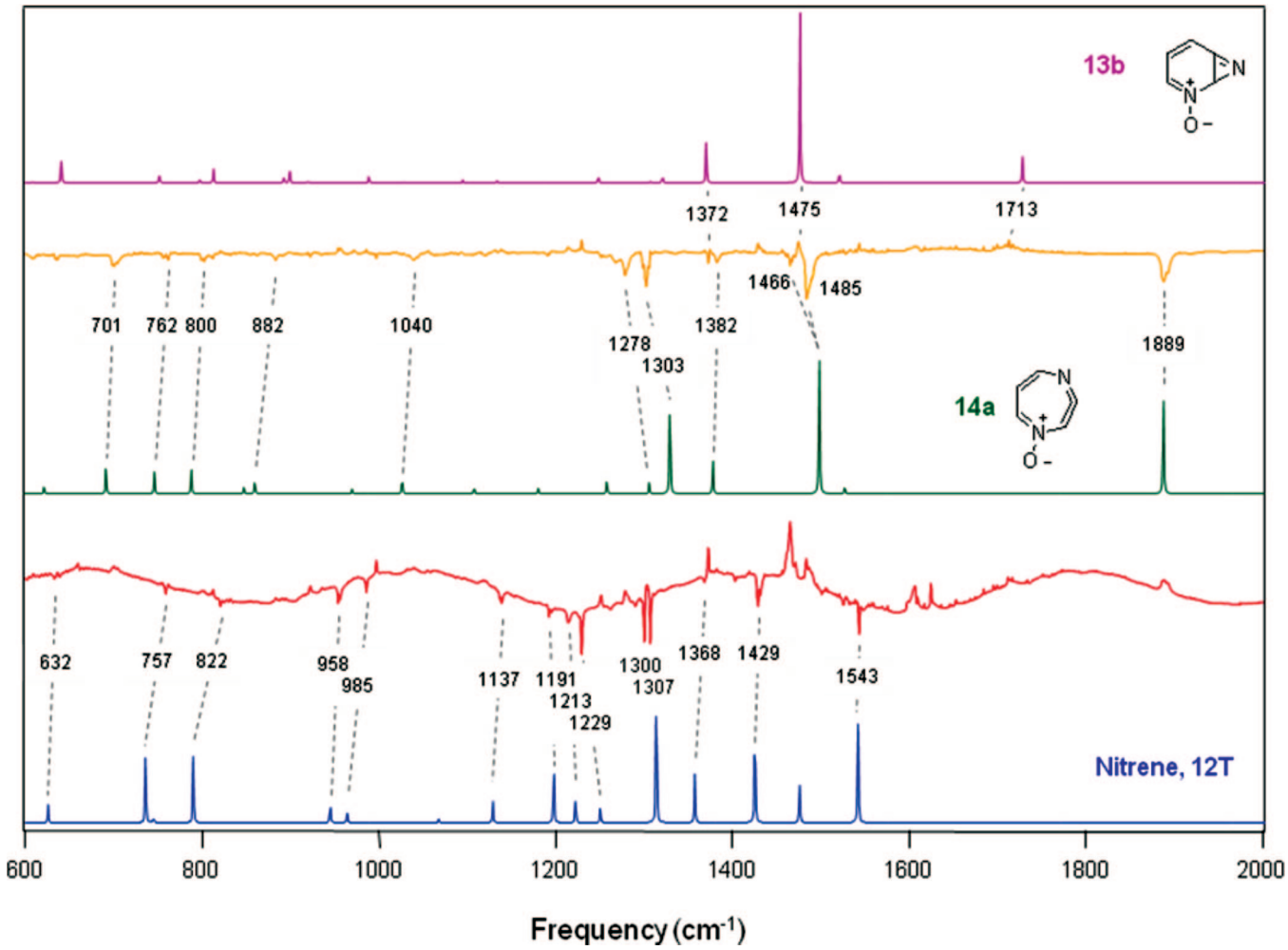

FIGURE 8. Differential IR spectra obtained following Ar matrix photolysis of a mixture of **12T**, **13b**, and **14a** (see Figure 7) at 530–680 nm (red), followed by photolysis at 395–450 nm (orange). Simulated spectra for **12T** (blue), **13b** (violet), and **14a** (green) are calculated at the B3LYP/6-31G* level of theory.

LUMO yielded a mixed singlet state with an S^2 expectation value of approximately 1, corresponding to a 50:50 mixture of open shell singlet and triplet states, as is typical for this methodology. The energy of the open shell singlet state was then estimated by the sum method (eq 1).[16]

$$E_{(OSS)}=2E_{(50:50mix)}-E_{(T)} \quad (1)$$

Natural population analysis (NPA)[24] was performed on critical intermediates.

UV–vis spectra for critical intermediates were simulated by calculating the vertical transition energies using time-dependent density functional theory.[25] In each case, the first 15 spin-allowed transitions were calculated at the TDB3LYP/6-31+G**//B3LYP/6-31G* level of theory, and the calculated transition energies and oscillator strengths are tabulated in the Supporting Information.

CASSCF calculations were also performed using GAUSSIAN 03 up to the CASSCF(10,9) level of theory. Geometry optimizations and frequencies were performed at the CASSCF(8,8)/6-31G* level of theory—vibrational frequencies and zero-point energies were unscaled. The orbitals used for the active space for each calculation are the same types as those used by previous workers[17] and are described in more detail in the Supporting Information. Single-point energies were calculated at the CASSCF(10,9)/6-31G*//CASSCF(8,8)/6-31G* level of theory to determine the effect of inclusion of the N−O π-orbital in the active space. Electron correlation effects were investigated by including an MP2 correction calculated at the CASSCF(8,8) MP2/6-31G* level of theory based on the CASSCF(8,8)/6-31G* geometry. Calculations were also performed on phenylnitrene as a comparator system where higher-level benchmark calculation data are available[17] (see the Supporting Information).

Experimental Methods

Compound **6** was prepared from the corresponding hydrazine, using the method of Itai and Kamiya,[10a] and recrystallized from acetone (see the Supporting Information). Compound **11** was prepared by oxidation of 3-azidopyridine.[10c,26] All solvents used in this study were obtained in spectroscopic purity from commercial sources, and were used without additional purification. The instruments used for characterization of organic compounds are described in the Supporting Information.

Glassy UV–vis Spectroscopy. Solutions of the azide in deoxygenated solvent (deoxygenation was achieved by bubbling argon

(24) (a) Reed, A. E.; Weinstock, R. B.; Weinhold, F. *J. Chem. Phys.* **1985**, *83*, 735. (b) Reed, A. E.; Weinhold, F.; Curtiss, J. A. *Chem. Rev.* **1988**, *88*, 899.

(25) (a) For examples, see: Bauernschmitt, R.; Ahlrichs, R. *Chem. Phys. Lett.* **1996**, *256*, 454. (b) Stratmann, E. R.; Scuseria, G. E.; Frisch, M. J. *J. Chem. Phys.* **1998**, *109*, 8218.

(26) Sawanishi, H.; Tajima, K.; Tsuchiya, T. *Chem. Pharm. Bull.* **1987**, *35*, 4101.

through the samples) in a 10 mm path length quartz cell were rapidly cooled to 77 K with liquid nitrogen in a quartz−Pyrex dewar. Solutions with a room temperature peak absorbance between 2.0 and 2.5 au were used. UV–vis spectra were obtained with a photodiode array spectrometer following irradiation with a broad spectrum medium pressure Hg vapor lamp—no wavelength filters were used in these experiments. Subsequent to photolysis, the glass was allowed to anneal, was revitrified, and a final spectrum was obtained.

Glassy Matrix EPR Spectroscopy. Solutions of azide were degassed (3-fold freeze–pump–thaw cycles) and sealed inside standard 4.0 mm o.d. quartz EPR sample tubes, which were sealed under vacuum. Samples were then frozen in liquid nitrogen in a quartz EPR X-band cavity finger Dewar and irradiated at 350 nm for 2–7 min using a carousel photoreactor. The dewar was placed into the EPR cavity and the spectrum obtained over a field range of 500–9500 gauss (modulation frequency 100 MHz, modulation amplitude 5–10 gauss, microwave power 6.8–19.3 mW, depending on the sample).

Argon Matrix Isolation Spectroscopy. The instrumental systems used in this study have been described previously.[27] To summarize, infrared and UV–vis spectra were obtained from argon matrices of the azides deposited on CsI plates cooled to 3–10 K using closed-cycle helium cryostats. IR spectra were collected through CsI windows, and UV–vis spectra were collected through sapphire windows. X-band EPR spectra were recorded at cryogenic temperatures by deposition of the argon matrices of the azides on an oxygen-free high-conductivity copper rod (75 mm length, 3 mm diameter) cooled by a closed-cycle 4.2 K cryostat. Photolysis of the samples was achieved using one of two methods:

(a) A high pressure mercury arc lamp, in combination with quartz optics and appropriate cutoff filters. KG1 filters were also used to absorb IR radiation from the lamps. This method provides broadband irradiation within the following bands, depending on the choice of filter: 295–320 nm, 395–450 nm, 530–680 nm.

(b) Monochromatic irradiation at 308 nm using an Xe−Cl excimer laser.

(27) (a) Sander, W.; Winkler, M.; Cakir, B.; Grote, D.; Bettinger, H. *J. Org. Chem.* **2007**, *72*, 715. (b) Dunkin, I. R. *Matrix Isolation Techniques*; Oxford University Press: Oxford, UK, 1998.

Acknowledgment. J.S.P. thanks the Lilly Endowment and the Research Corporation Cottrell College Science Award (CC-6456) for support of this project. W.S. thanks the Deutsche Forschungsgemeinschaft and the Fonds der Chemischen Industrie for financial support. T.E.M. thanks the Alexander von Humboldt Foundation. P.M.L. acknowledges NSF support for the UMass-Amherst EPR Facility (CHE 0443180).

Supporting Information Available: Synthetic methodologies for the starting material, additional spectroscopic data obtained in this study, and computational output in the form of optimized geometries, energies, and frequencies for species relevant to this study. This material is available free of charge via the Internet at http://pubs.acs.org.

JO8001936